OPTICAL AND INFRARED SPECTROSCOPY OF SN 1999ee AND SN 1999ex[1]

Mario Hamuy[2,3]

The Observatories of the Carnegie Institution of Washington, 813 Santa Barbara Street, Pasadena, CA 91101; mhamuy@ociw.edu

José Maza[3,4]

Departamento de Astronomía, Universidad de Chile, Casilla 36-D, Santiago, Chile; jose@das.uchile.cl

Philip A. Pinto

Steward Observatory, University of Arizona, Tucson, AZ 85721; ppinto@as.arizona.edu

M. M. Phillips

Carnegie Institution of Washington, Las Campanas Observatory, Casilla 601, La Serena, Chile; mmp@lco.cl

Nicholas B. Suntzeff, R. D. Blum, and K. A. G. Olsen

Cerro Tololo Inter-American Observatory, National Optical Astronomy Observatory,[5] Casilla 603, La Serena, Chile;
nsuntzeff@noao.edu, rblum@noao.edu, kolsen@noao.edu

David J. Pinfield[3]

Astrophysics Research Institute, Liverpool John Moores University, Twelve Quays House, Egerton Wharf, Birkenhead, CH41 1LD, UK;
dpi@astro.livjm.ac.uk

and

Valentin D. Ivanov, T. Augusteijn,[6] S. Brillant, M. Chadid, J.-G. Cuby, V. Doublier, O. R. Hainaut, E. Le Floc'h,
C. Lidman, Monika G. Petr-Gotzens,[7] E. Pompei, and L. Vanzi

European Southern Observatory, Alonso de Córdova 3107, Vitacura, Casilla 19001, Santiago 19, Chile; vivanov@eso.org, tau@ing.iac.es,
sbrillan@eso.org, mchadid@eso.org, jcuby@eso.org, vdoublie@eso.org, ohainaut@eso.org, elefloch@eso.org, clidman@eso.org,
mpetr@mpifr-bonn.mpg.de, epompei@eso.org, lvanzi@eso.org

ABSTRACT

We report optical and infrared spectroscopic observations of the Type Ia SN 1999ee and the Type Ib/c SN 1999ex, both of which were hosted by the galaxy IC 5179. For SN 1999ee we obtained a continuous sequence with an unprecedented wavelength and temporal coverage beginning 9 days before maximum light and extending through day 42. Before maximum light SN 1999ee displayed a normal spectrum with a strong Si II $\lambda 6355$ absorption, thus showing that not all slow-declining supernovae (SNe) are spectroscopically peculiar at these evolutionary phases. A comparative study of the infrared spectra of SN 1999ee and other Type Ia SNe shows that there is a remarkable homogeneity among the Branch-normal SNe Ia during their first 60 days of evolution. SN 1991bg–like objects, on the other hand, display spectroscopic peculiarities at infrared wavelengths. SN 1999ex was characterized by the lack of hydrogen lines, weak optical He I lines, and strong He I $\lambda\lambda 10830, 20581$, thus providing an example of an intermediate case between pure Ib and Ic supernovae. We conclude, therefore, that SN 1999ex provides the first clear evidence for a link between the Ib and Ic classes and that there is a continuous spectroscopic sequence ranging from the He-deficient SNe Ic to the SNe Ib, which are characterized by strong optical He I lines.

Key words: supernovae: individual (1999ee, 1999ex)

1. INTRODUCTION

The last 10 years have witnessed enormous progress in our knowledge of the optical properties of supernovae (SNe) of all types. However, it remains the case that comparatively little is known about these objects in near-infrared

(NIR) wavelengths. Given the rapid technological development of NIR light detection over recent years, in 1999 we started a program to obtain optical and NIR photometry and spectroscopy of nearby SNe ($z < 0.08$). So far this program, the Supernova Optical and Infrared Survey (SOIRS), has gathered high-quality observations for ~20 SNe, and we have reported results for the bright Type II SN 1999em (Hamuy et al. 2001). In this paper we report spectroscopic observations of two of the best-observed objects included in our program, the Type Ia SN 1999ee and the Type Ib/c SN 1999ex, which exploded in the same galaxy within 3 weeks of each other.

SN 1999ee was discovered by M. Wischnjewsky on a film taken on 1999 October 7.15 (JD 2,451,458.65) in the course of the El Roble survey (Maza & Hamuy 1999). The SN exploded $10''$ east and $10''$ south of the nucleus of the spiral galaxy IC 5179, a very active star-forming galaxy with a heliocentric redshift of 3,498 km s^{-1}. The optical spectrum taken on 1999 October 9.10 revealed the defining Si II $\lambda 6355$

feature of the Type Ia class (Maza & Hamuy 1999). The high expansion velocity of 15,700 km s^{-1} deduced from this line and the faint apparent magnitude at discovery ($\sim$17.5) indicated that this object had been found several days before maximum light. At the distance of the host galaxy SN 1999ee offered the promise to reach $V = 14.5$ about 10 days later, thus proving to be an excellent target for a detailed study of an SN Ia soon after the explosion, both at optical and IR wavelengths. This discovery occurred at the very beginning of one of the SOIRS follow-up runs, previously scheduled for 1999 October–November, so we decided to give first priority to SN 1999ee. The unique opportunity afforded by SN 1999ee led the director general of the ESO to allocate director's discretionary time to this project in order to secure the best possible data for SN 1999ee. As a result of this effort, we obtained a superb data set of optical/IR photometric and spectroscopic observations of the first 50 days of the evolution of SN 1999ee.

Three weeks after the discovery of SN 1999ee, a second SN exploded in IC 5179. The discovery of SN 1999ex was made by Martin et al. (1999) on 1999 November 9.51 UT (JD 2,451,492.01) in the course of the PARG Automated Supernova Search at Perth Observatory. They reported that the SN was not visible in a deep exposure taken on 1999 October 25.58 (estimated limiting magnitude 19) and that the object was slowly brightening. A spectrum taken on 1999 November 14.13 (Hamuy & Phillips 1999) showed that SN 1999ex had a close resemblance to the Type Ic SN 1994I taken near maximum light (Filippenko et al. 1995). This led us initially to classify SN 1999ex as a Ic event, although we believe that it should be typed as an intermediate Ib/c object (see § 4.2). As soon as this object was discovered, we decided to include it in our optical/IR spectroscopic follow-up.

The observations gathered for SNe 1999ee and 1999ex have unprecedented temporal and wavelength coverage and make it possible to carry out a detailed comparison with atmosphere models. In this paper we report the spectroscopic observations of SNe 1999ee and 1999ex, and we discuss these results. The spectra presented here are available in electronic form to other researchers.[8] Optical and IR photometry will be published and discussed in detail elsewhere by Stritzinger et al. (2002) and Krisciunas et al. (2002), respectively.

2. SPECTROSCOPIC OBSERVATIONS AND REDUCTIONS

We obtained optical and IR spectra of SNe 1999ee and 1999ex with the ESO NTT/EMMI/SOFI, the Danish 1.5 m/DFOSC spectrograph at La Silla and the VLT/ISAAC instrument at Cerro Paranal, between 1999 October 9 and November 28. We also obtained three optical spectra with the Cerro Tololo Inter-American Observatory (CTIO) 4 m telescope on 1999 October 9, the CTIO 1.5 m telescope on 1999 October 27, and the Las Campanas Dupont 2.5 m telescope on 1999 October 16. Table 1 gives the journal of the observations.

2.1. Optical Spectroscopy

The NTT observations comprised three different setups. We used the blue channel of EMMI equipped with a Tek CCD (1024 × 1024) and grating 5 (158 lines mm^{-1}), which,

in first order, delivered spectra with a dispersion of 3.5 Å pixel^{-1} and a useful wavelength range between 0.330 and 0.525 μm. With the red channel, CCD Tek 2048, and grating 13 (150 lines mm^{-1}) the dispersion was 2.7 Å pixel^{-1} and the spectral coverage included from 0.470 through 1.100 μm in first order. Since this setup had potential second-order contamination beyond $\sim$0.6 μm, we decided to take one spectrum with the OG530 filter and a second observation without the filter in order to provide an overlap with the blue spectrum. Thus a single-epoch observation comprised three spectra.

The observations with EMMI started with calibrations during the day time (bias and dome flat-field exposures). The night began with the observation of a spectrophotometric standard (from the list of Hamuy et al. 1994) through a wide slit of 10″, after which we observed the SNe with a slit of 1″. Before the discovery of SN 1999ex on 1999 November 9 we oriented the slit along the line connecting SN 1999ee and the host galaxy nucleus. On 1999 November 14 and 19, on the other hand, we oriented the slit along the two SNe in order to get simultaneous spectra. Since the air mass of our observations was always below 1.5, we do not expect serious systematic errors in the observed fluxes due to atmospheric refraction. We took two exposures of the SNe per spectral setup, each of the same length (typically 300–600 s). Immediately following this observation we observed a He-Ar lamp at the same position of the SNe and before changing the optical setup in order to ensure an accurate wavelength calibration. At the end of the night we observed a second flux standard.

We also used the Danish 1.5 m telescope and the DFOSC instrument at La Silla on five nights between 1999 October 20 and November 28, in order to improve the temporal coverage of our spectroscopic observations. In all cases we employed a 2K × 2K LORAL CCD and two different grisms to secure a spectral coverage comparable to that obtained with EMMI. With grism 3 (400 lines mm^{-1}) we covered a useful wavelength range between 0.33 and 0.66 μm with a dispersion of 2.3 Å pixel^{-1}. With grism 5 (300 lines mm^{-1}) we sampled the range between 0.53 and 0.98 μm at 3.1 Å pixel^{-1}. The red setup produced spectra with significant fringing beyond 0.75 μm which we did not attempt to remove. We observed the SNe with a slit of 2″. Although we did not rotate the slit along the parallactic angle, we obtained the first four spectra with air mass less than 1.1. The last spectrum taken on 1999 November 28, on the other hand, might suffer from different atmospheric refraction since we obtained it with an air mass between 1.4–2.0. We took two 1200 s exposures of the SNe per grism, followed by a He-Ne arc lamp exposure, and spectra of a flux standard with a 5″ slit.

We obtained a spectrum of SN 1999ee on 1999 October 9 (2 days after discovery) with the R-C spectrograph of the CTIO 4 m telescope, a 3K × 1K LORAL CCD, and grating KPGL-2 (316 lines mm^{-1}) in first order. We took one 1800 s exposure of the SN (through thick cirrus) with a 1″.5 slit oriented along the parallactic angle, a He-Ar lamp exposure, and spectra of three flux standards through a 10″ slit. The resulting SN spectrum had a dispersion of 1.9 Å pixel^{-1} and useful wavelength coverage of 0.33–0.87 μm. Second-order contamination was expected beyond 0.66 μm since we did not include a blocking filter in the optical path. We obtained another spectrum at CTIO with the 1.5 m telescope and the R-C spectrograph on 1999 October 27. In this case we used

TABLE 1

JOURNAL OF THE SPECTROSCOPIC OBSERVATIONS

UT Date	Phase[a] (days)	Julian Date −2,451,000	Observatory	Telescope	Instrument	Detector	Grating/Grism	Order	Wavelength (μm)	Dispersion (Å pixel^{-1})	Weather	Observer(s)
1999 Oct 09	−9	460.53	Paranal	VLT/Antu	ISAAC	Rockwell 1K	. . .	5, 4, 3, 2	0.98–2.50	2.9, 3.6, 4.7, 7.1	Clear	Hamuy, Lidman
1999 Oct 09	−9	460.53	Tololo	4 m	R-C Spec.	Loral 3K × 1K	KPGL-2	1	0.33–0.87	1.9	Cirrus	Maza
1999 Oct 11	−7	460.53	La Silla	NTT	EMMI	TEK 1024 + 2048	5, 13	1	0.33–1.01	2.7, 3.5	Clear	Hamuy, Doublier
1999 Oct 16	−2	460.53	Campanas	2.5 m	WFCCD	TEK 2048	Blue	. . .	0.36–0.92	3.0	Clouds?	Phillips
1999 Oct 18	0	460.53	La Silla	NTT	SOFI	Rockwell 1K	Red	. . .	1.50–2.53	10.2	Clear	Doublier, Maza
1999 Oct 18	0	460.53	La Silla	NTT	EMMI	TEK 1024 + 2048	5, 13	1	0.33–1.00	2.7, 3.5	Clear	Maza
1999 Oct 19	+2	460.53	Paranal	VLT/Antu	ISAAC	Rockwell 1K	. . .	5, 4, 3, 2	0.98–2.50	2.9, 3.6, 4.7, 7.1	Clear	Hamuy, Cuby, Petr
1999 Oct 20	+3	460.53	La Silla	D1.5 m	DFOSC	Loral 2K × 2K	3, 5	1	0.33–0.98	2.3, 3.1	. . .	Pompei
1999 Oct 22	+5	460.53	La Silla	NTT	SOFI	Rockwell 1K	Blue, Red	. . .	0.95–2.47	7.0, 10.2	Clear	Hainaut, Lefloc'h
1999 Oct 25	+8	460.53	La Silla	D1.5 m	DFOSC	Loral 2K × 2K	3, 5	1	0.33–0.98	2.3, 3.1	Clear	Augusteyn
1999 Oct 26	+8	460.53	La Silla	NTT	SOFI	Rockwell 1K	Blue, Red	. . .	0.95–2.46	7.0, 10.2	. . .	Hainaut, Vanzi
1999 Oct 27	+10	460.53	Tololo	1.5 m	R-C Spec.	Loral 1.2K × 0.8K	58	2	0.37–0.50	1.1	Clear	Olsen
1999 Oct 29	+12	460.53	La Silla	D1.5 m	DFOSC	Loral 2K × 2K	3, 5	1	0.34–0.98	2.3, 3.1	. . .	Augusteyn
1999 Nov 02	+15	460.53	Paranal	VLT/Antu	ISAAC	Rockwell 1K	. . .	5, 4, 3, 2	0.98–2.50	2.9, 3.6, 4.7, 7.1	Clear	Hamuy, Lidman, Petr
1999 Nov 03	+17	460.53	La Silla	NTT	EMMI	TEK 1024 + 2048	5, 13	1	0.33–1.01	2.7, 3.5	. . .	Maza
1999 Nov 06	+20	460.53	La Silla	NTT	SOFI	Rockwell 1K	Blue	. . .	0.94–1.65	7.0	Clear	Brillant
1999 Nov 06	+20	460.53	La Silla	D1.5 m	DFOSC	Loral 2K × 2K	3, 5	1	0.34–0.98	2.3, 3.1	Clear?	Augusteyn
1999 Nov 09	+23	460.53	La Silla	NTT	SOFI	Rockwell 1K	Blue, Red	. . .	0.95–2.51	7.0, 10.2	Clear	Hamuy, Brillant
1999 Nov 09	+23	460.53	La Silla	NTT	EMMI	TEK 1024 + 2048	5, 13	1	0.34–1.00	2.7, 3.5	Clear	Hamuy, Brillant
1999 Nov 14	+28	460.53	La Silla	NTT	SOFI	Rockwell 1K	Blue, Red	. . .	0.95–2.46	7.0, 10.2	Clear	Hamuy, Doublier
1999 Nov 14	+28	460.53	La Silla	NTT	EMMI	TEK 1024 + 2048	5, 13	1	0.34–1.00	2.7, 3.5	Clear	Hamuy, Doublier
1999 Nov 18	+32	460.53	Paranal	VLT/Antu	ISAAC	Rockwell 1K	. . .	5, 4, 3, 2	0.98–2.50	2.9, 3.6, 4.7, 7.1	Clear	Serv. Obs.
1999 Nov 19	+33	460.53	La Silla	NTT	EMMI	TEK 1024 + 2048	5, 13	1	0.34–1.00	2.7, 3.5	Clear	Hamuy, Doublier
1999 Nov 28	+42	460.53	Paranal	VLT/Antu	ISAAC	Rockwell 1K	. . .	5, 4, 3, 2	0.98–2.50	2.9, 3.6, 4.7, 7.1	Clear	Hamuy, Lidman, Chadid
1999 Nov 28	+42	460.53	La Silla	D1.5 m	DFOSC	Loral 2K × 2K	3, 5	1	0.40–0.98	2.3, 3.1	. . .	Pinfield

[a] Phase = days since B maximum (JD 2,451,469.0) of SN 1999ee.

a 1200 × 800 LORAL CCD, grating 58 (400 lines mm^{-1}) in second order, a 2″ slit, and a CuSO$_4$ order-blocking filter. The resulting spectrum had a dispersion of 1.1 Å pixel^{-1} and useful wavelength coverage of 0.37–0.50 μm. We obtained six 1200 s exposures of SN 1999ee at an air mass < 1.1, a He-Ar lamp image, and two spectra of flux standards.

We also obtained a spectrum of SN 1999ee on 1999 October 16 with the Las Campanas Dupont 2.5 m telescope and the Wide-Field CCD Spectrograph. We used a 2048 × 2048 TEK CCD, a blue grism and a 1″.5 slit. The resulting spectrum had a dispersion of 3 Å pixel^{-1} and useful wavelength coverage of 0.36–0.92 μm. Second-order contamination was expected beyond 0.66 μm since we did not use a blocking filter.

The reductions consisted in subtracting the overscan and bias from every frame. Next we constructed a normalized flat field from the quartz lamp image, duly normalized along the dispersion axis. We proceeded by flat-fielding all of the object frames and extracting one-dimensional spectra from the two-dimensional images. We followed the same procedure for the He-Ar frames, which we used to derive the wavelength calibration for the SNe. Then we derived a response curve from the two flux stars, which we applied to the SN spectra in order to get flux-calibrated spectra. From the pair of flux-calibrated spectra that we obtained for each spectral setup we removed cosmic rays and obtained a clean spectrum of each SN. The last step consisted in merging the spectra obtained with the different spectroscopic setups. To avoid discontinuities in the combined spectrum we gray-shifted the three spectra relative to each other using the overlap regions. Finally, we computed the synthetic V-band magnitude from the resulting spectra (following the precepts described in Appendix B of Hamuy et al. 2001), and we grayshifted them so that the flux level matched our observed V magnitudes. We checked the spectrophotometric quality of the spectra by computing BRI synthetic magnitudes and comparing them to the observed BRI magnitudes of Stritzinger et al. (2002). Excluding the spectra obtained on 1999 November 14, this test yielded the following mean differences: $B_{obs}-B_{syn}=-0.05 \pm 0.05$, $R_{obs}-R_{syn} = 0.00 \pm 0.07$, and $I_{obs}-I_{syn} = 0.00 \pm 0.09$, which implies that the relative spectrophotometry at these wavelengths is accurate to 10% or better. The November 14 spectrum, on the other hand, shows B fluxes that fall 0.35 mag lower than the photometric B magnitudes and I fluxes that exceed by 0.2 mag the observed broadband I magnitudes, perhaps owing to atmospheric refraction effects.

2.2. Infrared Spectroscopy

We obtained five IR spectra with the VLT/Antu telescope at Cerro Paranal, between 1999 October 9 and November 28 (see Table 1). We employed the IR spectroimager ISAAC (Moorwood 1997) in low resolution mode ($R \sim 500$), with four different gratings that permitted us to obtain spectra in the SZ, J, H, and K bands. We used these gratings in fifth, fourth, third, and second order, respectively, which yielded useful data in the spectral ranges 0.984–1.136, 1.109–1.355, 1.415–1.818, and 1.846–2.560 μm. The light detector was a Hawaii-Rockwell 1024 × 1024 array.

A typical IR observation started during daytime by taking calibrations. We began taking flat-field images using an internal source of continuum light. We obtained multiple on

and off image pairs with the same slit used during the night (0″.6). We then took Xe-Ar lamp images (with the lamp on and off) with a narrow slit (0″.3) in order to map geometric distortions. The observations of the SNe consisted in an ABBAAB cycle, where A is an image of the SNe offset by 70″ along the slit relative to the B image. This technique of nodding the objects along the slit allowed us to use the A image as an on-source observation and the B image as the off-source sky frame and vice versa. At each position we exposed for 240 s, conveniently split into two 120 s images in order to remove cosmic rays and bad pixels from the final spectra. After completing the ABBAAB cycle, we immediately obtained a pair of on-off arc lamp exposures without moving the telescope or changing optical elements to ensure an accurate wavelength calibration. We then switched to the next grating and repeated the above object-arc procedure until completing the observations with the four setups. For flux calibration we decided to observe a bright solar-analog star, close in the sky to the SNe to minimize variations in the atmospheric absorptions (Maiolino et al. 1996). The selected star was Hip 109508, of spectral type G3 V, $V = 8.0$, $B-V = 0.59$, and located only 3° from the SNe. In this case we took two AB pairs for each grating. To avoid saturating the detector, we took the shortest possible exposures (1.77 s) allowed by the electronics that controlled the detector. Since the minimum time required before offsetting the telescope was ~60 s, we took 10 exposures at each position, which provided an exceedingly good signal-to-noise ratio (S/N) for the flux standard.

Our data reduction procedures were explained in detail by Hamuy et al. (2001), so we include here only a brief summary. After dividing all of the object images by a normalized flat field, we performed a first-order sky subtraction by subtracting the A images from the B exposures (and vice versa). We then shifted the A-B image relative to the B-A image in the spatial direction until matching the two spectra, and we added the shifted A-B image to the B-A image so that the resulting frame lacked any sky background, except for the pixel-to-pixel fluctuations expected from photon statistics and readout noise. We then extracted one-dimensional spectra of the objects from the sky-subtracted frames, making sure to subtract residual DC offset and galaxy light from a window adjacent to the object. For flux calibration we adopted the technique described by Maiolino et al. (1996), which consists in dividing the spectrum of interest by a solar-type star to remove the strong telluric IR features and multiplying the resulting spectrum by the solar spectrum to eliminate the intrinsic features (pseudonoise) introduced by the solar-type star. Before using the solar spectrum, we convolved it with a kernel function to reproduce the spectral resolution of the solar-analog standard Hip 109508, shifted it in wavelength according to the radial velocity (68 km s^{-1}) of Hip 109508, and scaled it down to the equivalent of $V = 8.0$, which corresponds to the observed magnitude of Hip 109508. This technique worked very well to remove telluric lines. On the other hand, it introduced a small systematic error in the flux calibration of the SN due to departures between the solar spectrum and the actual spectral energy distribution of the solar-analog standard. According to atmosphere models the difference in continuum flux for stars with $T_{eff} = 5500$ and 6000 K (which correspond to spectral types G8 V–F9 V, Gray & Corbally 1994) is smaller than 10% in the NIR region. A G3 V star such as Hip 109508 has nearly the same spectral type of the

Sun, so its effective temperature must be close (within ±100 K) to that of the adopted solar model. Hence, the flux difference between the solar-analog standard and the adopted spectrum should be less than 10%. The $B-V = 0.59$ color of Hip 109508 suggests little or no reddening so the relative spectrophotometry is probably accurate to 5% or better.

The result of these operations were four spectra covering the SZ, J, H, and K bands, which we combined into one final IR spectrum for each SN. Given the significant overlap of the SZ- and J-band spectra, we were able to grayshift the J spectrum relative to the SZ spectrum. Then we used our broadband JHK magnitudes to grayshift the individual spectra.

On six occasions we used the NTT/SOFI instrument at La Silla in service observing mode, in order to complement the IR spectroscopic follow-up. We employed a Hawaii-Rockwell 1024 × 1024 light detector, and the blue and red grisms that permitted us to obtain spectra in the ranges 0.95–1.64 μm and 1.53–2.52 μm, with resolutions of 7.0 and 10.2 Å, respectively. We obtained the spectra with slit widths between 0″.6 and 1″. We nodded the objects along the slit, after exposing for 150 s at each position. We completed several pairs of AB observations for the SNe, took Xe-Ne arc images at the position of the targets, and observed the flux standard Hip 109508. We reduced these data following the same procedure explained above for ISAAC. The large overlap of 1.53–1.64 μm between the blue and red spectra allowed us to grayshift the red spectra relative to blue spectra, except on 1999 October 18 when we were only able to obtain the red spectrum. Finally, we shifted the resulting spectra using the observed JHK magnitudes (Krisciunas et al. 2002).

3. RESULTS

3.1. *SN 1999ee*

Before analyzing the spectroscopic observations it proves necessary to mention the photometric properties of SN 1999ee. A detailed discussion of the photometric observations can be found in Stritzinger et al. (2002). In brief, the decline rate of $\Delta m_{15}(B) = 0.94$ puts SN 1999ee in the group of slowest-declining SNe Ia. After correcting the observed magnitudes for K terms and dust extinction and assuming a Hubble constant of 63 km s^{-1} Mpc^{-1} (Phillips et al. 1999), SN 1999ee had a peak visual magnitude of $M_V = -19.95$ (JD 2,451,471.7). These values lie comfortably well with the peak magnitude–decline rate relation for SNe Ia (Phillips et al. 1999). This analysis reveals that SN 1999ee was a luminous Type Ia event and a very interesting object to check the claim by Li et al. (2001b) that slow-declining events display spectroscopic peculiarities before maximum light.

Figure 1 displays the optical spectra of SN 1999ee in the rest frame of the SN, after correcting the observed spectra for the 3498 km s^{-1} recession velocity of the host galaxy. We also dereddened the spectra assuming a Galactic reddening of $E(B-V) = 0.02$ (Schlegel et al. 1998), and a host galaxy reddening of $E(B-V) = 0.30$ derived from the SN optical colors (Stritzinger et al. 2002) and optical/IR colors (Krisciunas et al. 2002). The strongest telluric lines are indicated with the circled plus sign. The first optical spectrum, taken on JD 2,451,460.56 (9 days before maximum), exhibited a blue continuum and the characteristic P Cygni profile of the Si II $\lambda6355$ line of SNe Ia. Other prominent features in this
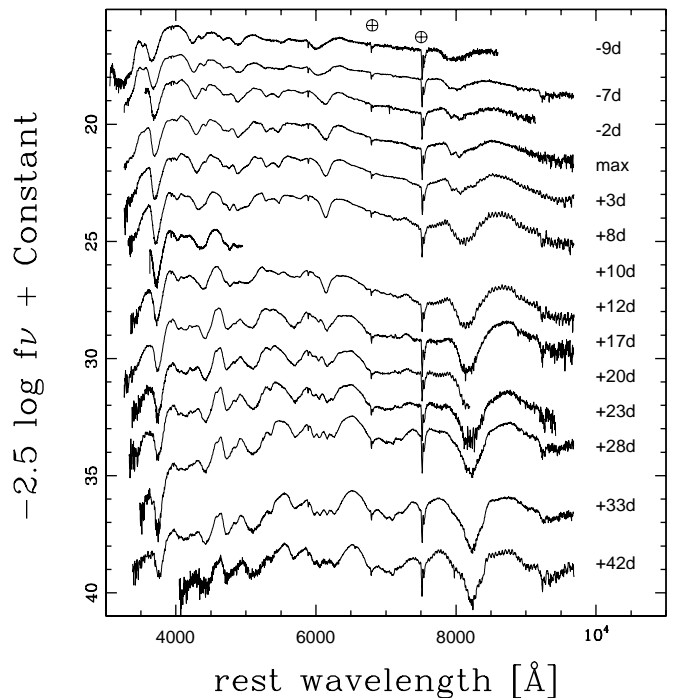

FIG. 1.—Optical spectroscopic evolution of SN 1999ee in AB magnitudes. Time (in days) since B maximum is indicated for each spectrum. The circled plus signs symbols show the main telluric features.

spectrum were the absorption at ~3200 Å attributed to Co II, the Ca II H and K $\lambda\lambda3934$, 3968 blend, Mg II $\lambda4481$, the blend of lines attributed to Fe II, Si II, S II around 4550–5050 Å, and the Ca II $\lambda\lambda8498$, 8542, 8662 triplet. The presence of the Na I D $\lambda\lambda5890$, 5896, Ca II $\lambda3934$, and Ca II $\lambda3968$ interstellar lines with equivalent widths of 2.3, 0.8, and 0.6 Å, respectively, revealed a nonnegligible amount of absorption in the host galaxy, which agrees with the color analysis of SN 1999ee. By maximum light the W-shaped S II $\lambda\lambda5454$, 5640 feature was well developed and the Ca lines were significantly stronger. Si II $\lambda4129$ was already present, although it was quite weak. The Si II $\lambda5972$ line also was weak relative to Si II $\lambda6355$. Nugent et al. (1995) defined the parameter $\mathcal{R}$(Si II) as the relative fluxes of this pair of lines and found a tight correlation with the SN luminosity. In this case we obtained $\mathcal{R}$(Si II) = 0.23, which corresponds to the value of a luminous SNe Ia, in good concordance with the decline rate of $\Delta m_{15}(B) = 0.94$ and the peak magnitudes derived from the photometric observations. By day 20 the spectrum was much redder. The Si II $\lambda6355$ line was very weak, the Ca triplet had a pronounced P Cygni profile, and the region between 4000–5500 Å was dominated by strong features due to Fe II transitions. The absorption attributed to Na I D $\lambda\lambda5890$, 5896 was very prominent. Overall, these data showed that SN 1999ee was a genuine Type Ia event with the usual spectral features of other normal SNe Ia, usually known as Branch-normal (Branch et al. 1993).

Figure 2 presents the expansion velocities derived from the absorption minima of Si II $\lambda6355$, after correcting for the recession velocity of the host galaxy. Apparently, the velocity derived from Si II $\lambda6355$ decreased rapidly from 16,000 to 10,000 km s^{-1} between days -9 and -2, after which the velocity decreased slowly. For comparison, we
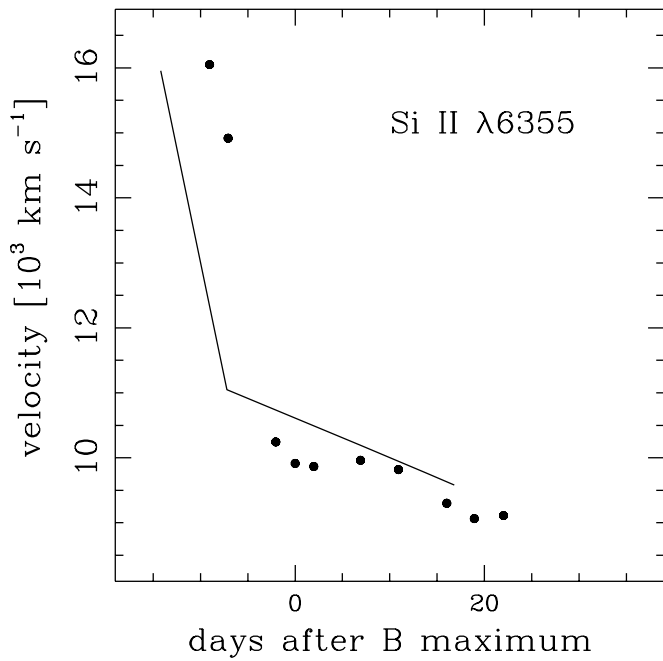
FIG. 2.—Expansion velocities derived from the absorption minima of Si II $\lambda6355$ for SN 1999ee, after correcting for the recession velocity of the host galaxy. The solid line corresponds to SN 1990N.

include as solid line the velocities for SN 1990N, which was also caught several days before maximum (Leibundgut et al. 1991). Both SNe showed an inflection in the velocity curve. Before maximum, however, the expansion of SN 1999ee was somewhat higher compared with contemporary velocities of SN 1990N. At maximum light and later times, on the other hand, both SNe had similar velocities.
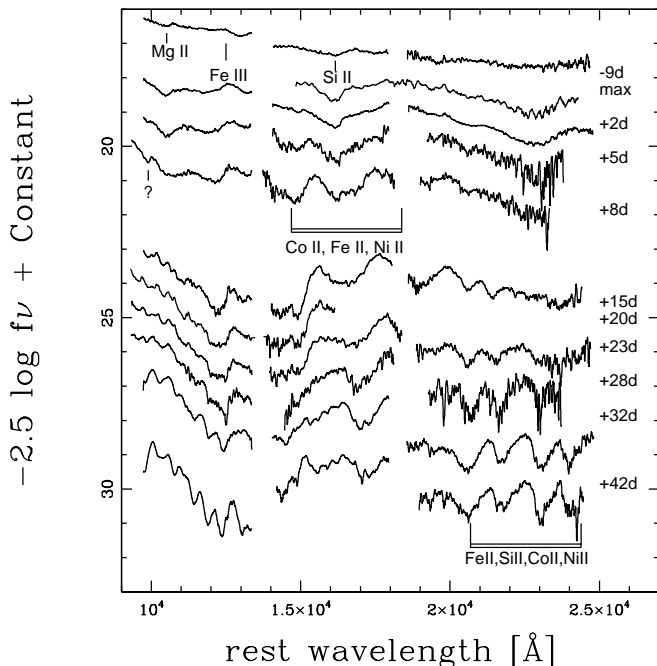
FIG. 3.—IR spectroscopic evolution of SN 1999ee in AB magnitudes. The most prominent features are labeled. Time (in days) since B maximum is indicated for each spectrum.

Figure 3 shows the resulting rest-frame IR spectra of SN 1999ee. The first spectrum, taken 9 days before maximum, was quite featureless. A weak absorption line could be seen at 10520 Å, with a weak emission component that seemed to constitute a P Cygni profile. This feature was observed for the first time in an early-time spectrum of SN 1994D and was tentatively identified as due to either He I $\lambda10830$ or Mg II $\lambda10926$ (Meikle et al. 1996). According to the atmosphere models computed by Wheeler et al. (1998), this feature should be due to Mg II, since the amount of He in their models is not sufficient to form a line. This implies that the minimum of the Mg absorption had an expansion velocity of 11,100 km s^{-1}. An emission due to Fe III (Rudy et al. 2002) was also present around 12550 Å. There was an indication of a P Cygni profile with the absorption minimum at 16160 Å and peak emission at 16840 Å. This feature was also present in the SN 1994D spectrum. The theoretical modeling of Wheeler et al. suggests that this line is due to Si II, although it might have a Fe II component (Axelrod 1980). At longer wavelengths the spectrum is even more featureless, except for a small P Cygni line with a minimum at 19590 Å and peak at 20440 Å. The emission component was also noted in SN 1994D and was attributed to Si III by Wheeler et al.

By maximum light the Mg II $\lambda10926$, Fe III, and Si II feature near 16500 Å became more prominent, and a peak developed around 18100 Å. One week past maximum the spectrum was dramatically different and became dominated by strong absorption/emission features. The Mg II $\lambda10926$ line disappeared and a weak feature at 10000 Å became evident, possibly forming a P Cygni profile. The most remarkable features were the strong and wide (FWHM $\sim$ 12,000 km s^{-1}) peaks attributed to blends of Co II, Fe II, and Ni II at 15500 and 17500 Å (Wheeler et al. 1998). Two weeks after maximum these peaks developed even further and new peaks appeared at 19900 and 21000 Å. A series of unidentified absorptions also could be observed in the J band at 10400, 10700, and 11100 Å. One month after maximum two additional broad emission peaks became evident at 22500 and 23600 Å, which, according to Wheeler et al., are caused by iron-group elements (Co, Ni) as well as intermediate-mass elements with appreciable contribution from Si. While the broad emissions appeared to redshift significantly as the SN evolved, the features that we identify as absorptions did not show any appreciable change in velocity.

3.2. SN 1999ex

Figure 4 displays the optical spectra of SN 1999ex in the SN rest frame. The first optical spectrum, obtained on JD 2,451,496.62 (1 day before B maximum), was characterized by a reddish continuum and several broad absorption/emission features due to Ca II H and K $\lambda\lambda3934$, 3968, Fe II, Mg I, Na I D $\lambda\lambda5890$, 5896, Si II $\lambda6355$, and the Ca triplet with a clear P Cygni profile. We also found convincing evidence for He I $\lambda\lambda6678$, 7065 with expansion velocities of 6000 km s^{-1} (similar to velocities displayed by the Fe, Mg, Na, Si, and O lines). It is possible that the feature at $\sim$4400 Å, usually attributed to a blend of Mg II and Fe II, had a contribution due to the He I $\lambda4471$. Likewise, the feature at $\sim$4800 Å could be a blend of Fe II $\lambda4924$ and He I $\lambda4921$, while the Na I D $\lambda\lambda5890$, 5896 doublet could have a contribution from He I $\lambda5876$. Interstellar lines due to Na I D $\lambda\lambda5890$, 5896, Ca II $\lambda3934$, and Ca II $\lambda3968$ were observed in absorp-
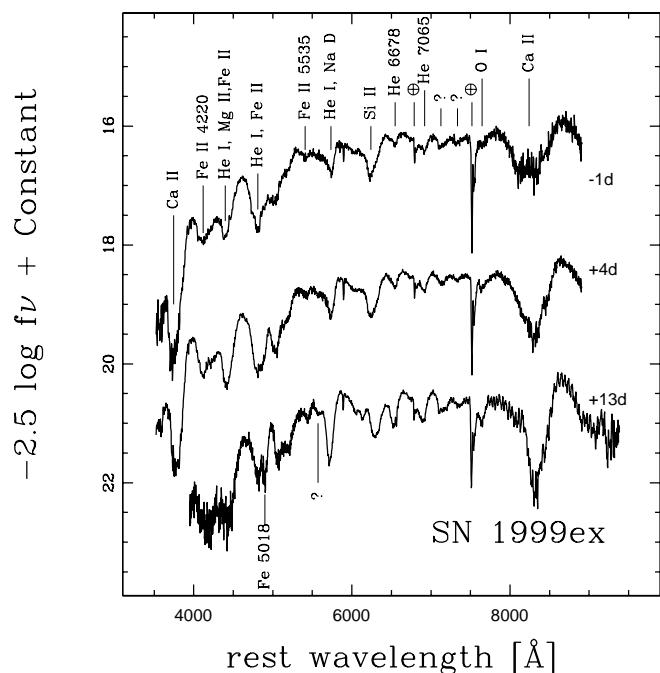
FIG. 4.—Optical spectroscopic evolution of SN 1999ex in AB magnitudes. Time (in days) since B maximum is indicated for each spectrum. The most prominent features are labeled, and the main telluric features are marked with a circled plus sign.
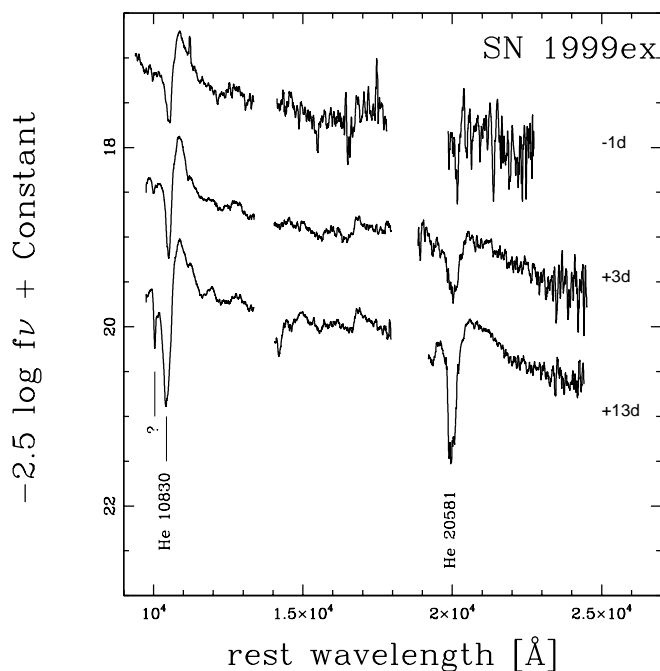

FIG. 5.—IR spectroscopic evolution of SN 1999ex in AB magnitudes. The two most prominent features are due to He I, while the absorption at 10000 Å remains unidentified. Time (in days) since B maximum is indicated for each spectrum.

tion with equivalent widths of 2.8, 1.8, 0.9 Å at the wavelengths corresponding to the rest frame of the host galaxy. According to the correlation between equivalent widths and reddening for Galactic stars (Munari & Zwitter 1997), SN 1999ex was reddened by $E(B-V) \sim 1.0 \pm 0.15$. However, there appears to be a significant departure of SNe from this calibration (Hamuy et al. 2001), so this estimate is very uncertain.

The first spectrum of SN 1999ex bore a close resemblance to that of SN 1994I. Filippenko et al. (1995) argued that SN 1994I was a Type Ic event on the grounds that this object (1) did not show evidence for hydrogen lines (ruling out a Type II event), (2) had a Si II $\lambda6355$ line more subtle than in classical SNe Ia, and (3) He I $\lambda5876$ was absent or weak (and blended with Na D) (ruling out a Type Ib event). Based on the resemblance between these two spectra, we initially classified SN 1999ex as a Type Ic SN (Hamuy & Phillips 1999). However, the relatively stronger He lines displayed by SN 1999ex suggest that this object could well be an intermediate case between the Ib and Ic subclasses (we will return to this point in § 4.2). During the following 2 weeks the SN spectrum evolved slowly, and most of the lines became stronger.

Figure 5 displays the IR spectra of SN 1999ex in the SN rest frame. The most prominent feature in these spectra is the P Cygni profile of He I $\lambda10830$, which was also observed in SN 1994I. The minimum of the absorption yields an expansion velocity of 8000 km s^{-1}, in good agreement with the values derived from the optical spectra. The other evident feature is the P Cygni profile due to He I $\lambda20581$, with the same expansion velocity. An unidentified absorption at 9970–10045 Å can be clearly seen, which should have a rest wavelength between 10200–10260 Å. A few weak unidentified lines can be seen also in the H band.

4. DISCUSSION

4.1. *SN 1999ee*

Although Type Ia SNe display a large degree of spectroscopic homogeneity, there are several examples of SNe with spectral peculiarities. Different subclasses have been identified including SN 1991T–like objects (Phillips et al. 1992), Branch-normal SNe (Branch et al. 1993), and SN 1991bg–like events (Phillips et al. 1987; Filippenko et al. 1992; Leibundgut et al. 1993). Recently the Lick Observatory Supernova Survey (LOSS) produced a SN sample with well-understood selection effects (Li et al. 2001a), which permitted them to assess the intrinsic peculiarity rate of SNe Ia (Li et al. 2001b). This study showed that the sample of nearby SNe Ia comprises 20%, 64%, and 16% of 1991T-like, normal, and 1991bg-like objects, respectively.

Li et al. (2001a) defined a normal SN as one with prominent features due to Si II $\lambda6355$, Ca II H and K $\lambda\lambda3934$, 3968, as well as additional lines of S II, O I, and Mg II around maximum light. The designation SN 1991T in such work is not strictly correct, since the prototype of the 1991T class defined by Li et al. (2001b) is SN 1999aa. While SN 1999aa's main difference relative to normal SNe is just a relative weakness of the Si II $\lambda6355$ feature before maximum, which becomes almost indistinguishable from normal SNe after peak (see Fig. 5 of Li et al. 2001b), SN 1991T was a much more extreme event, in the sense that the premaximum spectrum did not display the Ca II H and K $\lambda\lambda3934$, 3968 blend shown by Branch-normal SNe and also because it remained spectroscopically distinct several days after maximum (Phillips et al. 1992). For the sake of clarity, in what follows we refer to the 1991T-like events of Li et al. as 1999aa-like objects. The distinguishing feature of SN 1991bg–like objects is the Ti II absorption around 4100–

4000 Å. There are many examples of intermediate-class objects, which suggests a continuous spectral sequence among SNe Ia.

Because 1999aa-like events display slow-declining light curves ($\Delta m_{15}(B) \leq 1.0$) and high peak luminosities, and 1991bg-like SNe show fast decline rates ($\Delta m_{15}(B) \geq 1.7$) and low peak luminosities, it is interesting to ask whether the photometric behavior can be used to predict spectroscopic peculiarities. As a slow-declining ($\Delta m_{15}(B) = 0.94$) and luminous ($M_V = -19.75$) event observed well before maximum light, SN 1999ee provides a good opportunity to investigate whether or not all luminous SNe display spectroscopic peculiarities before peak. To examine this point in detail Figure 6 (*top*) shows a comparison of the spectrum of SN 1999ee taken 9 days before B maximum with that of three other SNe, including SN 1999aa, with a decline rate of $\Delta m_{15}(B) = 0.75$ (Krisciunas et al. 2000), the Calán/Tololo SN 1992bc with $\Delta m_{15}(B) = 0.87$ (Hamuy et al. 1996), and the normal SN 1990N with $\Delta m_{15}(B) = 1.07$ (Leibundgut et al. 1991; Lira et al. 1998). While SN 1999aa lacked the Si II $\lambda 6355$ feature compared with the Branch-normal SN 1990N, both SN 1992bc and SN 1999ee displayed strong and well-defined Si features as early as 10 days before peak. This shows that *not all slow-decliners are spectroscopically peculiar before maximum light*. As mentioned above, 1999aa-like events show a normal spectrum at peak brightness, which can be clearly appreciated in the bottom panel of Figure 6 from the spectra of SN 1999aa and SN 1999ee. The fact that the spectral differences displayed by the luminous SNe are only limited to the very first days of evolution suggests that the 1999aa-like and the Branch-normal SNe

(represented here by SN 1999ee) are apparently similar explosions and that spectral diversity at early times probably reflects small differences in mixing or other chaotic behaviors, rather than fundamental differences in the character of the explosions.

There are a handful of IR spectra published for SNe Ia (Meikle et al. 1996; Bowers et al. 1997; Hernández et al. 2000; Jha et al. 1999; Rudy et al. 2002). Höflich et al. (2002) recently observed SN 1999by and assembled the first continuous sequence of IR spectra for an SN Ia, extending from 3 days before maximum through day +15 after peak. To our knowledge the IR spectra of SN 1999ee—extending from day −9 to +42—constitute the most complete IR spectroscopic sequence of an SN Ia, and its Branch-normal nature makes it an ideal object in which to study the homogeneity of this class of objects at these wavelengths. We proceed now to address this issue from a sample of five SNe Ia encompassing a wide range in decline rates and optical spectroscopic properties. The sample comprises the Branch-normal SN 1999ee, SN 1998bu (Jha et al. 1999; Hernández et al. 2000), and SN 1994D (Meikle et al. 1996), with $\Delta m_{15}(B) = 0.94$, 1.01, 1.32, respectively (Phillips et al. 1999).[9] We also include SN 1999by [$\Delta m_{15}(B) = 1.90$], which had optical spectra showing resemblance to SN 1991bg (Garnavich et al. 2001), and SN 2000cx [$\Delta m_{15}(B) = 0.93$], which shared some of the spectroscopic peculiarities displayed by SN 1999aa–like events (e.g., weak Si II $\lambda 6355$) before maximum and a " sui generis " postmaximum behavior, owing to unusually strong Fe III and weak Fe II lines (Li et al. 2001c).

Figure 7 (*top*) compares premaximum spectra of SN 2000cx, 1999ee, 1994D, and 1999by. The resemblance between the two Branch-normal SNe (1999ee and 1994D) is remarkable. The largest, yet subtle, difference was the Mg II $\lambda 10926$ feature, which was narrower and deeper in SN 1994D. The expansion velocities derived from the absorption minimum was quite similar, $\sim 10{,}500$ km s^{-1}. Both the Si II and Si III features near 16500 and 20000 Å were clearly present in both SNe. With the exception of the high Mg II velocity ($\sim 20{,}000$ km s^{-1}), SN 2000cx showed a normal featureless spectrum. Since magnesium is destroyed by oxygen burning, it is expected in material that experiences burning at the lowest densities near the surface. The high Mg velocity led Rudy et al. (2002) to conclude that nuclear burning in SN 2000cx extended farther out than in normal SNe, though it is equally likely that in this supernovae a blob containing carbon burning products drifted closer to the surface than in some other SNe Ia. The greater luminosity and slower decline of SN 2000cx argue for greater ^{56}Ni production, and this would manifest itself also in greater excitation in the ejecta. Indeed, SN 2000cx showed an emission feature at 12500 Å attributed to Fe III $\lambda\lambda 12786$, 12920, 13003 (Rudy et al. 2002), which was also present in the normal SN 1999ee but at a lower strength, a weaker than normal Si II feature near 16500 Å, and a stronger Si III line around 20000 Å.

SN 1999by showed a premaximum spectrum noticeably different than that of normal SNe. The main difference was due to C I and O I lines, which were clearly absent in the spectra of other SNe. Höflich et al. (2002) suggested that
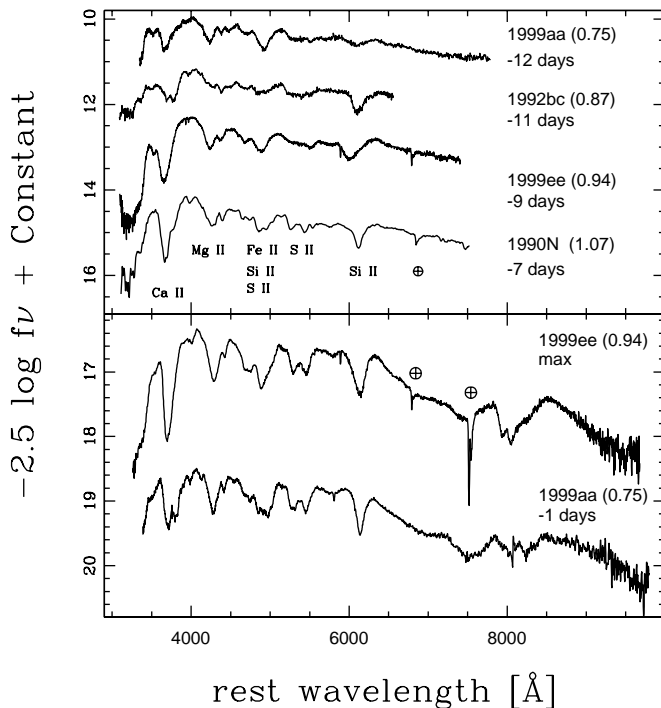

FIG. 6.—*Top*: Comparison of the optical spectra of three slow-declining SNe Ia and the Branch-normal SN 1990N obtained about 10 days before B maximum. The spectra have been shifted with respect to each other by arbitrary amounts to facilitate comparison. Given in parenthesis are the decline rates $\Delta m_{15}(B)$ for each SN. *Bottom*: Same as above, but for SN 1999aa and SN 1999ee near maximum light.

[9] We include in this comparison two spectra of SN 1998bu obtained by one of us (R. D. B.) with the CTIO 4 m Infrared Spectrograph on 1998 May 16 (3 days before B maximum) and June 3 (15 days after peak).
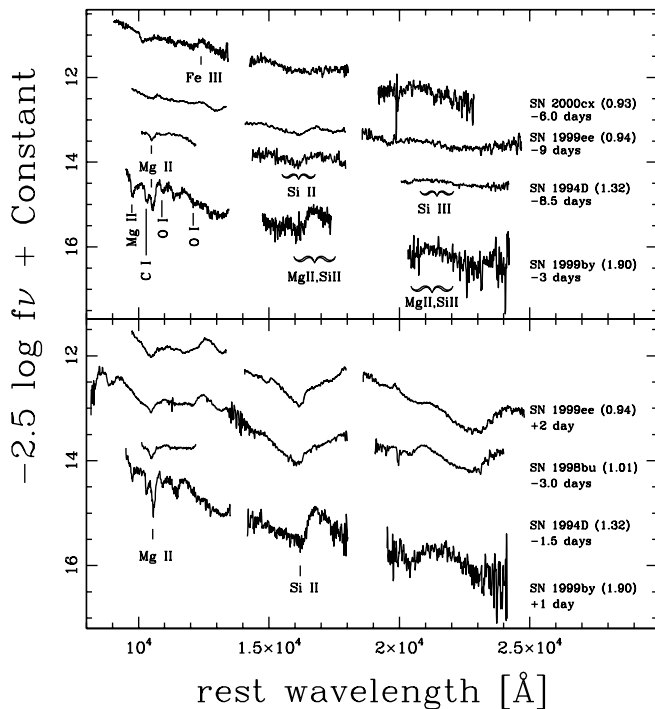
Fig. 7.—Comparison of the premaximum and maximum-light IR spectra of SNe 1994D, 1998bu, 1999by, 1999ee, and 2000cx. Time (in days) since B maximum is indicated for each spectrum, along with the decline rates $\Delta m_{15}(B)$.

nuclear burning in SN 1999by did not extend as far out as in normal SNe Ia. It is possible, however, that the presence of the C I and O I lines was due to a lower excitation evidenced by the smaller ^{56}Ni production, the low luminosity, and fast decline of SN 1999by. The spectral differences are particularly evident in the J band. The Mg II $\lambda10926$ feature was deeper than normal, although its velocity of $\sim10,000$ km s^{-1} was similar to that observed in normal SNe. In the H band SN 1999by showed a strong broad-emission feature due to a blend of Si II and Mg II lines, which was also present in the other SNe, but with a lower strength, presumably due to a weaker contribution from Mg II. The K-band spectrum is also bumpier than normal due to Mg II lines.

Around maximum light the Mg II $\lambda10926$ feature was present in all three normal SNe (1999ee, 1998bu, and 1994D) with similar strengths and profiles (*bottom*, Fig. 7). Meikle et al. (1996) noted that the absorption minimum of the Mg II line did not show a shift in wavelength during the premaximum evolution of SN 1994D, as opposed to the optical lines, which all redshifted with time as the photosphere receded through the ejecta. We confirmed the absence of any significant Doppler shift in Mg II from SN 1999ee, which, according to Wheeler et al. (1998), was due to the fact that the photosphere had already receded below the inner edge of the magnesium layer at this early phase. It is interesting to note the absence in these spectra of the Ca II line near 11500 Å, a feature predicted by the models of Wheeler et al. (1998), which proves to be a useful diagnostic of the location of the transition layer between complete and incomplete silicon burning. The Si II absorption near 16500 Å and the spectral features in the K band were visible in the normal SNe 1999ee and 1998bu with a high degree of simi-

larity. The premaximum spectral peculiarities of SN 1999by mentioned above were still evident near maximum light.

Figure 8 compares the postmaximum spectra available to us. Two weeks after peak the two normal SNe, 1999ee and 1998bu, displayed an impressive spectral homogeneity, with strong peaks and valleys at 15000–17000 Å and 22000–26000 Å due to Fe II, Co II, Ni II, and Si II. The presence of Fe II, Co II, Ni II, and Si II is due to the ionization dropping predominantly to these ions, which happen to have strong lines in the near IR. The spectral differences of the fast-declining SN 1999by persisted at this epoch. While its J spectrum had contributions from Ca II lines (Höflich et al. 2002) that were absent in SNe 1999ee and 1998bu, the broad emission around 15000–17000 Å was weaker than normal. At later epochs the spectra of SNe 1999ee and 1998bu became much more complicated, yet their similarity remained remarkable.

As a result of this observational campaign we obtained the most complete optical/IR observations of a Type Ia SN, with an unprecedented wavelength and temporal coverage beginning nine days before maximum light. Moreover, since we were able to obtain the IR spectra within 1 or 2 days of the optical spectra, it was possible to combine these observations, as shown in Figure 9. This exercise revealed the excellent agreement between the optical and IR fluxes, a result that proved possible by synthesizing broadband magnitudes and adjusting the flux scales according to the observed magnitudes. This optical/IR sequence shows that, while the premaximum optical spectrum was dominated by strong P Cygni profiles of intermediate-mass elements, such as Ca II, Si II, Mg II, S II, the IR was characterized by a smooth, almost featureless continuum. By maximum light, on the other hand, the IR spectrum was already dominated
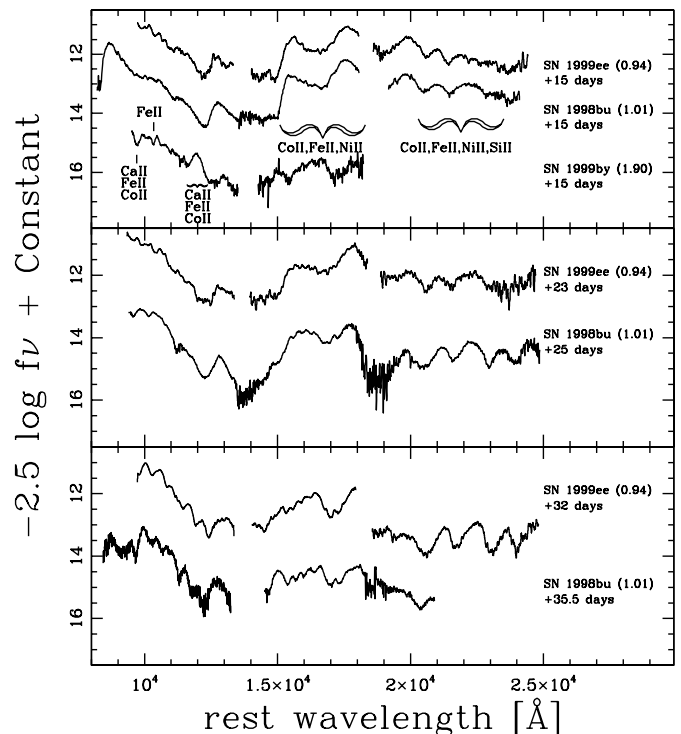

Fig. 8.—Comparison of the postmaximum IR spectra of SNe 1998bu, 1999by, and 1999ee. Time (in days) since B maximum is indicated for each spectrum, along with the decline rates $\Delta m_{15}(B)$.
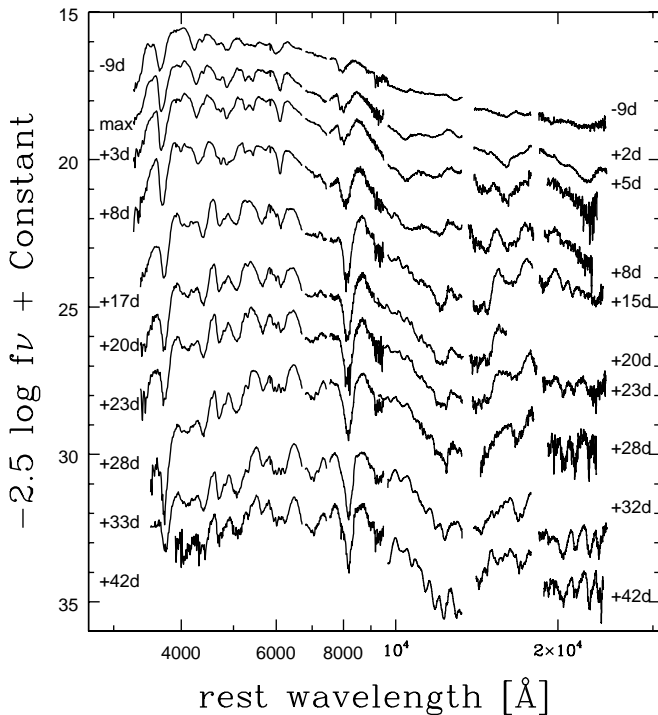
FIG. 9.—Combined optical and IR spectra of SN 1999ee in AB magnitudes. Time (in days) since *B* maximum is indicated for each spectrum.

by broad features, and 1 week later the IR flux was mostly powered by emission lines of iron group elements, such as Co II, Fe II, and Ni II (freshly synthesized in the innermost layers of the ejecta), which were particularly prominent in the *H* and *K* bands. At the same time a dramatic flux dip around 12000 Å began to develop. Previous spectroscopic observations have already revealed this *J*-band deficit in other SNe Ia (Bowers et al. 1997), which is responsible for the red *J*−*H* color displayed by SNe Ia after maximum light (Elias et al. 1985).

This spectral sequence lends support to the suggestion by Spyromilio, Pinto, & Eastman (1994) and Pinto & Eastman (2000) that the " photosphere " recedes rapidly to the center of the supernova in the IR, while at optical wavelengths the greater opacity arising from the higher spectral density of lines keeps the photosphere at higher velocities. Emission at longer wavelengths increases after maximum light as a result of a shift in ionization to more neutral species, which have greater emissivity in the near IR. In this model the *J*-band deficit is due to the relative absence of lines (and hence opacity) in the 12000 Å region, rather than increasing opacity. Likewise, the secondary maxima exhibited by the *JHK* light curves ∼30 days after *B* maximum (Elias et al. 1981; Elias et al. 1985; Jha et al. 1999; Hernández et al. 2000; Krisciunas et al. 2000) are due to the increasing release of energy through lower optical depth IR transitions. The prominent postmaximum emission features displayed by SN 1999ee in the *H* and *K* bands lend support to this picture.

4.2. *SN 1999ex*

SNe are classified according to their spectral features near maximum light (Filippenko 1997). Type II SNe are characterized by prominent hydrogen features and are believed to

arise from the core collapse of massive (>8–10 $M_\odot$) stars. The common feature in all Type I SNe is the lack of hydrogen spectral lines. The strong Si II λ6355 is the defining feature of SNe Ia. Their occurrence in all types of stellar environments has led to the general consensus that the progenitors of SNe Ia are white dwarfs that undergo thermonuclear disruption after a period of mass transfer from binary companions. The proximity of SNe Ib and Ic to massive star formation regions (Van Dyk et al. 1996), on the other hand, provides evidence that these objects result from the core collapse of massive stars. The lack of hydrogen in their spectra is attributed to the loss of their outer hydrogen envelopes by stellar winds or mass transfer to binary companions. There is growing evidence for a close physical connection between SNe II and SNe Ib from the observations of SNe 1987K, 1993J, and 1996cb, which evolved from SNe II at early epochs to SNe Ib at later times (Filippenko 1988; Filippenko et al. 1993; Qiu et al. 1999). The distinguishing difference between Type Ib and Ic SNe are the *optical* He I lines, which are conspicuous in SNe Ib and weak or absent in SNe Ic. It is still a matter of debate whether SNe Ic constitute an extreme case of SNe Ib or a completely separate class of objects. The apparent absence of He in the spectra of SNe Ic motivated the idea that the progenitors of these objects could be nearly bare C + O cores of massive stars (Wheeler & Harkness 1990), which lose most of their helium by binary transfer or strong stellar winds. However, Woosley et al. (1995) showed that helium stars could be the progenitors of both SNe Ib and SNe Ic. They showed that the presence or absence of He I lines in the spectrum is determined primarily by the amount of mixing, not the amount of helium present—greater mixing of radioactive material increases the excitation of helium, leading to stronger lines.

Significant effort over recent years has been put into determining the presence of helium in the spectra of SNe Ic in order to better understand the nature of these objects. A detailed inspection of the spectra of the Type Ic SN 1994I led Filippenko et al. (1995) to conclude that weak He I lines were probably present in the optical region and that He I λ10830 was very prominent, although its Doppler shift implied an unusually high expansion velocity of ∼16,600 km s^{-1}. Clocchiatti et al. (1996) confirmed these observations and found evidence that He I λ5876 was also present in SN 1994I, with a blueshift of ∼17,800 km s^{-1}. They also reported high-velocity He I λ5876 in the spectra of the three best-observed Type Ic SNe (1983V, 1987M, and 1988L), which led them to conclude that most, and probably all, SNe Ic provide evidence for optical He I lines. This conclusion, however, was recently questioned by Millard et al. (1999) and Baron et al. (1999) by means of spectral synthesis models, which showed that the IR feature near 10250 Å could be accounted for with lines of C I and Si I. Moreover, Baron et al. (1999) argued that the feature attributed to He I λ5876 in the spectrum of SN 1994I could be a blend of other species. Evidently, there is no consensus yet about the presence or absence of He in the spectra of SNe Ic.

Recently Matheson et al. (2001) compiled and analyzed a large collection of spectra of SNe Ib and Ic. This study showed no compelling evidence for He in the spectra of SNe Ic and no gradual transition from the Ib to the Ic class, which supported the idea that these objects are produced by different progenitors.

Our optical spectra of SN 1999ex provide evidence for He I absorptions of moderate strength in the optical region,
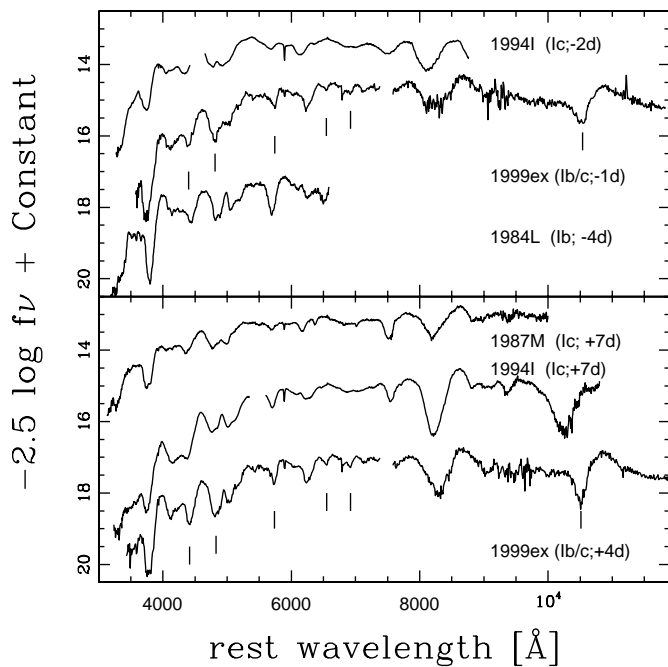
FIG. 10.—Comparison of near-maximum spectra of the Type Ib/c SN 1999ex with the prototype of the Ib class SN 1984L, and the Type Ic SNe 1994I and 1987M. Tick marks indicate the He I lines in the SN 1999ex spectra. The strengths of the He lines gradually increase from the Type Ic to the Ib SN, and SN 1999ex appears to bridge the separation between these two subclasses.

thus suggesting the existence of an intermediate Ib/c case. To illustrate this point, in Figures 10 and 11 we show a comparison between SN 1999ex, the best-observed Type Ic SN 1994I, and the prototypes of the Ib (SN 1984L, Harkness et al. 1987) and Ic class (SN 1987M, Filippenko, Porter, & Sargent 1990). The near-maximum spectra (top, Fig. 10) reveal
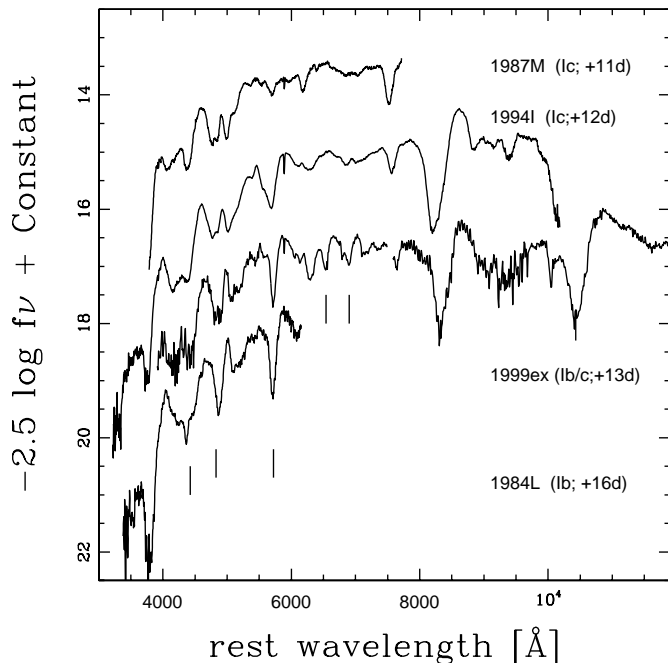
FIG. 11.—Same comparison as in Fig. 10, but for spectra taken 2 weeks past maximum.

a gradual increase in the strength of all He lines (*indicated with tick marks*) from the Ic to the Ib class. In the bottom panel of Figure 10 (1 week past maximum) it is possible to see that, even though the spectra of the Type Ic SNe 1994I and 1987M are quite similar, SN 1994I shows deeper troughs at the wavelengths of the He I lines, especially at 4471, 4921, and 5876 Å. The spectrum of SN 1994I obtained 2 weeks past maximum (Fig. 11) is particularly interesting, as it provides good evidence that the He I λ5876 line was indeed present in the spectrum of SN 1994I with a higher expansion velocity than the Na I D λ5893 doublet. This was also noted by Filippenko et al. (1995), who quoted an expansion velocity of $\sim$16,600 km s^{-1} for the He line (see also Clocchiatti et al. 1996 for a detailed discussion). Overall, Figures 10–11 reveal that there is a smooth spectroscopic sequence ranging from the He deficient Type Ic SNe 1987M and 1994I, the Type Ib/c SN 1999ex, and the Type Ib SN 1984L that is characterized by strong optical He lines. We conclude, therefore, that SN 1999ex provides the first evidence for a link between the Ib and Ic classes and that there is a continuous sequence of SNe Ib and Ic objects.

Special attention must be paid to the IR feature near 11000 Å, which was very prominent in SNe 1999ex and 1994I. As mentioned above the definitive identity of this feature in SN 1994I is still uncertain: it could be accounted for with lines of C I and Si I (Millard et al. 1999; Baron et al. 1999) or with high-velocity He I λ10830 (Filippenko et al. 1995; Clocchiatti et al. 1996). If the feature in SN 1999ex were He I λ10830, it would imply a moderate velocity of 6,000–8,000 km s^{-1}, which matches very well the velocities derived from the Fe, Na, and Si lines. The presence of the He I λ20581 with the same expansion velocity (see Fig. 5) suggests that the IR feature in SN 1999ex was indeed due to He I λ10830. Altogether our IR spectra of SN 1999ex provide unambiguous proof that He was present in the atmosphere of this intermediate Ib/c object. A detailed atmosphere model could be very useful for placing limits on the He mass in the ejecta of SN 1999ex and constraining the nature of its progenitor. As suggested by Clocchiatti et al. (1996), the presence of highly blueshifted He I λ5876 in SN 1994I suggests that the IR feature was also due to He I λ10830. If so, the difference in He velocities between SNe 1994I and 1999ex might prove an interesting clue to the underlying physics of the atmospheres of this class of objects. Further optical/IR spectroscopy and photometry will lead us to better understand the atmospheres of SNe Ib and Ic.

Finally, given that the IR spectra were obtained within one day from the optical spectra, we were able to combine these observations. Figure 12 shows the resulting spectra and the excellent agreement between the optical and IR fluxes. Note the prominent He I $\lambda\lambda$10830, 20581 features.

4.3. *Maximum-Light Optical/IR Spectra of Supernovae*

In the course of the SOIRS program we obtained high-quality spectroscopy of the Type II SN 1999em (Hamuy et al. 2001). Figure 13 compares maximum-light spectra of the Type II SN 1999em, the Type Ib/c SN 1999ex, and the Type Ia SN 1999ee. This figure permits one to compare the different characters of the main classes of SNe, all the way from 3,000 to 25,000 Å. The Type II is distinguished by prominent hydrogen Balmer and Paschen lines. It also shows the P Cygni profile of the He I λ10830 transition. The Type II
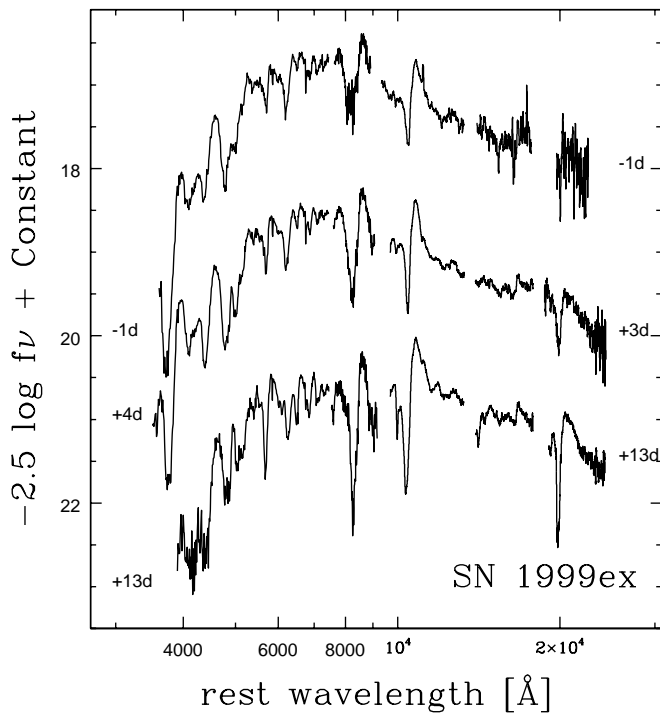
FIG. 12.—Combined optical and IR spectra of SN 1999ex in AB magnitudes. Days since *B* maximum are indicated next to each spectrum.

FIG. 13.—Combined optical and IR maximum-light spectra of the Type II SN 1999em, the Type Ib/c SN 1999ex, and the Type Ia SN 1999ee.

spectrum is also characterized by a strong, well-defined continuum. The Type Ib/c is characterized by the strong He I $\lambda\lambda10830$, 20581 lines in the IR, the He I $\lambda5876$ line in the optical, and other lines in the optical due to singly ionized Ca, Fe, Mg, and Si and neutral Na and O. It is interesting to note that, while both Type II and Type Ib/c show strong He I $\lambda10830$, only the Type Ib/c shows a significant He I $\lambda20581$ feature. The spectrum of SN 1999ex also seems to show evidence for a photosphere throughout the duration of the observations. This is clearly different than what is observed for SNe Ia, and more like a Type II. Finally, the Type Ia at the bottom of this figure is characterized by strong Si II $\lambda6355$ and other intermediate-mass elements, as well as by the absence of hydrogen and helium.

5. CONCLUSIONS

The observations obtained for SN 1999ee constitute the most complete spectral and temporal coverage ever achieved for a SN Ia. Its Branch-normal character makes it an ideal reference for comparative studies of SNe Ia.

Before maximum light SN 1999ee displayed a normal spectrum with a strong Si II $\lambda6355$ absorption, thus showing that not all slow-declining SNe are spectroscopically peculiar at these evolutionary phases. We conclude that the photometric properties of luminous SNe Ia cannot be used to predict spectroscopic peculiarities.

From a comparison of the IR spectra of SN 1999ee and other SNe Ia that encompass a wide range in decline rates, we find that there is a remarkable homogeneity among the Branch-normal SNe Ia during their first 60 days of evolution. Although the slow-decliner luminous SN 2000cx showed a premaximum featureless IR spectrum similar to
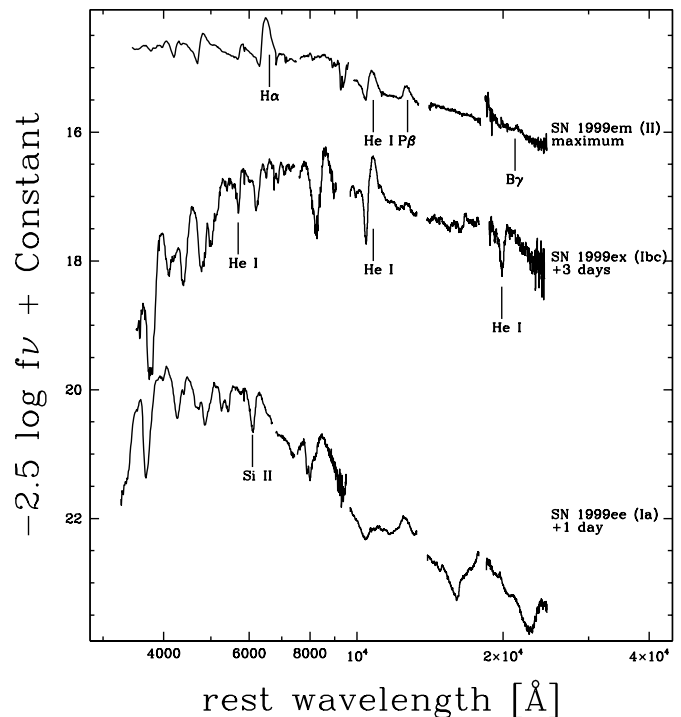
that of normal SNe, the Mg II $\lambda10926$ line was characterized by a high expansion velocity. The fast-declining subluminous SN 1999by was noticeably different than the other SNe at all epochs. This study reveals that the spectroscopic peculiarities displayed by SN 1991bg–like objects at optical wavelengths are also present in the IR.

The fortunate occurrence of SN 1999ex within 3 weeks and in the same galaxy that hosted SN 1999ee permitted us to obtain optical and IR spectroscopy of a Ib/c event. SN 1999ex was characterized for the lack of hydrogen lines, weak optical He I lines, and strong He I $\lambda\lambda10830$, 20581, thus providing an example of an intermediate case between pure Ib and Ic SNe. We conclude, therefore, that SN 1999ex provides first clear evidence for a link between the Ib and Ic classes and that there is a continuous spectroscopic sequence ranging from the He-deficient SNe Ic to the SNe Ib, which are characterized by strong optical He I lines.

REFERENCES

Axelrod, T. S. 1980, Ph. D. thesis, Univ. California, Santa Cruz
Baron, E., Branch, D., Hauschildt, P. H., Filippenko, A. V., & Kirshner, R. P. 1999, ApJ, 527, 739
Bowers, E. J. C., Meikle, W. P. S., Geballe, T. R., Walton, N. A., Pinto, P. A., Dhillon, V. S., Howell, S. B., & Harrop-Allin, M. K. 1997, MNRAS, 290, 663
Branch, D., Fisher, A., & Nugent, P. 1993, AJ, 106, 2383
Clocchiatti, A., Wheeler, J. C., Brotherton, M. S., Cochran, A. L., Wills, D., Barker, E. S., & Turatto, M. 1996, ApJ, 462, 462
Elias, J. H., Frogel, J. A., Hackwell, J. A., & Persson, S. E. 1981, ApJ, 251, L13
Elias, J. H, Matthews, K., Neugebauer, G., & Persson, S. E. 1985, ApJ, 296, 379
Filippenko, A. V. 1988, AJ, 96, 1941
———. 1997, ARA&A, 35, 309
Filippenko, A. V., Matheson, T., & Ho, L. C. 1993, ApJ, 415, L103
Filippenko, A. V., et al. 1995, ApJ, 450, L11
———. 1992, AJ, 104, 1543
Filippenko, A. V., Porter, A. C., & Sargent, W. L. W. 1990, AJ, 100, 1575
Garnavich, P. M., et al. 2001, ApJ, submitted (astro-ph/0105490)
Gray, R. O., & Corbally, C. J. 1994, AJ, 107, 742
Hamuy, M., et al. 1996, AJ, 112, 2408
Hamuy, M., & Phillips, M. M. 1999, IAU Circ. 7310
Hamuy, M., et al. 2001, ApJ, 558, 615
Hamuy, M., Suntzeff, N. B., Heathcote, S. R., Walker, A. R., Gigoux, P., & Phillips, M. M. 1994, PASP, 106, 566
Harkness, R. P., et al. 1987, ApJ, 317, 355
Hernández, M., et al. 2000, MNRAS, 319, 223
Höflich, P., Gerardy, C. L., Fesen, R. A., & Sakai, S. 2002, ApJ, 568, 791
Jha, S., et al. 1999, ApJS, 125, 73
Krisciunas, K., Hastings, N. C., Loomis, K., McMillan, R., Rest, A., Riess, A. G., & Stubbs, C. 2000, ApJ, 539, 658
Krisciunas, K., et al. 2002, in preparation
Leibundgut, B., Kirshner, R. P., Filippenko, A. V., Shields, J., C., Foltz, C. B., Phillips, M. M., & Sonneborn, G. 1991, ApJ, 371, L23
Leibundgut, B., et al. 1993, AJ, 105, 301
Li, W., Filippenko, A. V., & Riess, A. G. 2001a, ApJ, 546, 719
Li, W., Filippenko, A. V., Treffers, R. R., Riess, A. G., Hu, J., & Qiu, Y. L. 2001b, ApJ, 546, 734
Li, W., et al. 2001c, PASP, 113, 1178
Lira, P., et al. 1998, AJ, 115, 234
Maiolino, R., Rieke, G. H., & Rieke, M. J. 1996, AJ, 111, 537
Martin, R., Williams, A., Woodings, S., Biggs, J., & Verveer, A. 1999, IAU Circ. 7310
Matheson, T., Filippenko, A. V., Li, W., Leonard, D. C., & Schields, J. C. 2001, AJ, 121, 1648
Maza, J., & Hamuy, M. 1999, IAU Circ. 7272
Meikle, W. P. S, et al. 1996, MNRAS, 281, 263
Millard, J., et al. 1999, ApJ, 527, 746
Moorwood, A. F. 1997, in Proc. SPIE, 2871, 1146
Munari, U., & Zwitter, T. 1997, A&A, 318, 269
Nugent, P., Phillips, M., Baron, E., Branch, D., & Hauschildt, P. 1995, ApJ, 455, L147
Phillips, M. M., Lira, P., Suntzeff, N. B., Schommer, R. A., Hamuy, M., & Maza, J. 1999, AJ, 118, 1766
Phillips, M. M., et al. 1987, PASP, 99, 592
Phillips, M. M., Wells, L. A., Suntzeff, N. B., Hamuy, M., Leibundgut, B., Kirshner, R. P., & Foltz, C. B. 1992, AJ, 103, 1632
Pinto, P. A., & Eastman, R. G. 2000, ApJ, 530, 757
Qiu, Y., Li. W., Qiao, Q., & Hu, J. 1999, AJ, 117, 736
Rudy, R. J., Lynch, D. K., Mazuk, S., Venturini, C. C., Puetter, R. C., & Höflich, P. 2002, ApJ, 565, 413
Schlegel, D. J., Finkbeiner, D. P., & Davis, M. 1998, ApJ, 500, 525
Spyromilio, J., Pinto, P. A., & Eastman, R. G. 1994, MNRAS, 266, L17
Stritzinger, M., et al. 2002, in preparation
Van Dyk, S. D., Hamuy, M., & Filippenko, A. V. 1996, AJ, 111, 2017
Wheeler, J. C., & Harkness, R. P. 1990, Rep. Prog. Phys., 53, 1467
Wheeler, J. C., Höflich, P., Harkness, R. P., & Spyromilio, J. 1998, ApJ, 496, 908
Woosley, S. E., Langer, N., & Weaver, T. A. 1995, ApJ, 448, 315